Investigation of 3D printed polymer-based heat dissipator for GaN transistors

Tony Gerges, Alexandre Marie, Thilini Wickramasinghe, Philippe Lombard, Marie Levêque, Stéphane Lips, Valérie Sartre, Bruno Allard, Michel Cabrera

Investigation of 3D printed polymer-based heat dissipator for GaN transistors

Tony Gerges[1], Alexandre Marie[2], Thilini Wickramasinghe[1], Philippe Lombard[1], Marie Levêque[2], Stéphane Lips[2], Valérie Sartre[2], Bruno Allard[1], Michel Cabrera[1]
[1]Univ Lyon, INSA Lyon, Université Claude Bernard Lyon 1, École Centrale de Lyon, CNRS, Ampère, UMR5505, 69621 Villeurbanne, France
[2]Univ Lyon, INSA Lyon, CNRS, CETHIL UMR5008, F-69621 Villeurbanne, France
Phone: +33 (0) 472-438238
Fax: +33 (0) 472-438530
E-Mail: tony.gerges@insa-lyon.fr
http:/www.ampere-lab.fr
https://cethil.insa-lyon.fr

Keywords

≪Thermal design≫, ≪Plastronics≫, ≪DC-DC power converter≫, ≪Two-Phase cooling≫, ≪Packaging≫

Abstract

GaN transistors are limited in their operational capabilities due to some limitations, of which the thermal management aspects. Until now, most of the existing heat-dissipator systems using additive manufacturing (AM) are based on a metallic finned heat sink, which is heavy and has a relatively high thermal resistance. Heat dissipation based on a phase change as operated in heat pipes is more efficient. Such heat sinks have been experimented with metals or ceramics and not by now with polymers. However, this may be of great interest. The use of polymer may enable reducing weight and cost of the thermal device. It may allow also improving the chemical compatibility of the heat pipe material and fluid, as this is often a severe issue. This work presents a characterization of a 3D-printed polymer-based heat pipe evaporator intended for GaN transistors. The electronic copper circuit on the polymer surface is created using plastronics technology. The metallized circuit presents an adequate electrical conductivity. The thermal characterization performed with the HFE 7000 fluid, shows that it is actually possible to cover the entire heated polymer wall with active nucleation sites once the full developed nucleate boiling regime is reached. The heat conduction through the insulating polymer wall appears as the limiting phenomenon for heat transfer.

Introduction

GaN transistors are widely used in high-density power converters. Their performances have pushed the operating frequency whilst keeping low additional losses. The small footprint of the devices is nonetheless a limitation regarding an efficient cooling approach [1, 2], which is one major issue towards high density.

In this context, additive manufacturing (AM) offers an alternative technique for a heat-sink implementation. Certain limitations imposed by conventional manufacturing could be over-passed as well as it allows an easy customized design to suit the thermal requirement of the

system. This would improve globally the packaging issue. Additive Manufacturing is also known to reduce the lead-time, the time-to-market and increases the innovation speed with respect to application-specific problems [3]. Many types of cooling systems have been reported using AM and specifically metal additive manufacturing (MAM), largely studied because of the high thermal conductivity of the metals. Experiments using graphene have also been reported [4] but may not emerge as a cost-effective solution in a near future.

Recent studies describe the use of MAM to create cooling systems for power electronics with the fabrication of a hybrid microjet-microchannel heat sink [5]. Other systems have been reported such as: low-mass thermal management system based on titanium-water heat pipes with grooves [6], vapor chamber with porous structure distributed through the chamber and 3D printed with stainless steel [7], 3D printed loop heat-pipe with stainless steel [8] or the design of an air-cooled heat-sink [9]. However, MAM requires inert atmosphere to prevent the oxidation of the metal during printing which explains the high cost fabrication. MAM approach mimics in fact the design of standard cooling strategies and the benefit in terms of power density is not significant. This is particularly important in the case of medium-power applications where losses are limited and a breakthrough in power density is required by the industry.

In other respects, studies report the fabrication of heat transfer systems using polymer AM. The polymer systems have the advantage of being electrical insulators, which allows an easy implementation of electrical circuits. Low-power and medium-power applications call for converters fabricated on FR4 polymer substrate. There is a possibility for co-fabricating the cooling assistance of the devices along with the substrate dedicated to electrical interconnections.

Michalak et al. [10] report recently a heat sink fabricated using stereolithography (SLA), one of the major AM techniques for polymer, and applying impingement-cooling principles. A multilayer system is combining SiC devices within PCB and ceramics substrates and SLA printing. Wei et al. [11] present a similar example and their results show that a 3D-printed microfluidic heatsink improves the cooling performances by a factor of 5, compared to a standard air-cooled heat sink. The system footprint is preserved at the expense of an extra thickness. No additional discrete thermal device is considered. The reduction in the Bill of Material (BoM) is a benefit as well as the possible reduction in failure modes. More recently, Air Jet Impingement Cooling of GaN devices was designed [12]. Finally, the print orientation effects of 3D-printed composite heat sinks were discussed in [13].

To the best of our knowledge, only one article has so far reported a full 3D-printed system to support a power converter [14], i.e. implementing electrical interconnections, landing pads for discrete electronic devices and thermal assistance, all into one design and a unified fabrication step. The circuit board and the heat sink of the buck converter reported in [11] were obtained using AM technology. However, the prototype had its own limitations due to the low performances of the involved materials and an imperfect design of the thermal part. Results are nonetheless promising.

The paper reports here the investigation of a polymer-based heat-dissipator for GaN transistors using AM and plastronics technologies. 3D Plastronics, which is also called 3D Molded Interconnect devices (3D-MID) [15], is used to obtain a highly conductive metallized circuit at the surface of a 3D polymer without using any additional layer such as FR4. It is important to investigate the possibility of using 3D-printed polymer walls as an efficient pool-boiling substrate and the interest of such a system for cooling a GaN-transistor power core in a medium-power converter. The next section details the design of the thermal approach. A demonstrator is then characterized from thermal point of view. The results are discussed in the perspective of a power core.

3D-printed evaporator design

In a first step, the evaporator consists in an axisymmetric object represented in isometric section view as pictured in Fig. 1(a). The thermally active area is a planar surface of 1 mm thick (chosen as the minimal value for sufficient mechanical rigidity of the wall) and 40 mm in diameter. On

the periphery of the boiling surface, thicker walls are used to ensure enough mechanical rigidity for the prototype. A vehicle electronic circuit encompassing GaN transistors as well as gate drivers is soldered directly inside the evaporator (Fig. 1(b)) using a standard brazing process in a first step. The polymer layer thickness under the GaN transistors is reduced to 0.5 mm to reduce the thermal interface impedance (Fig. 1(c)).

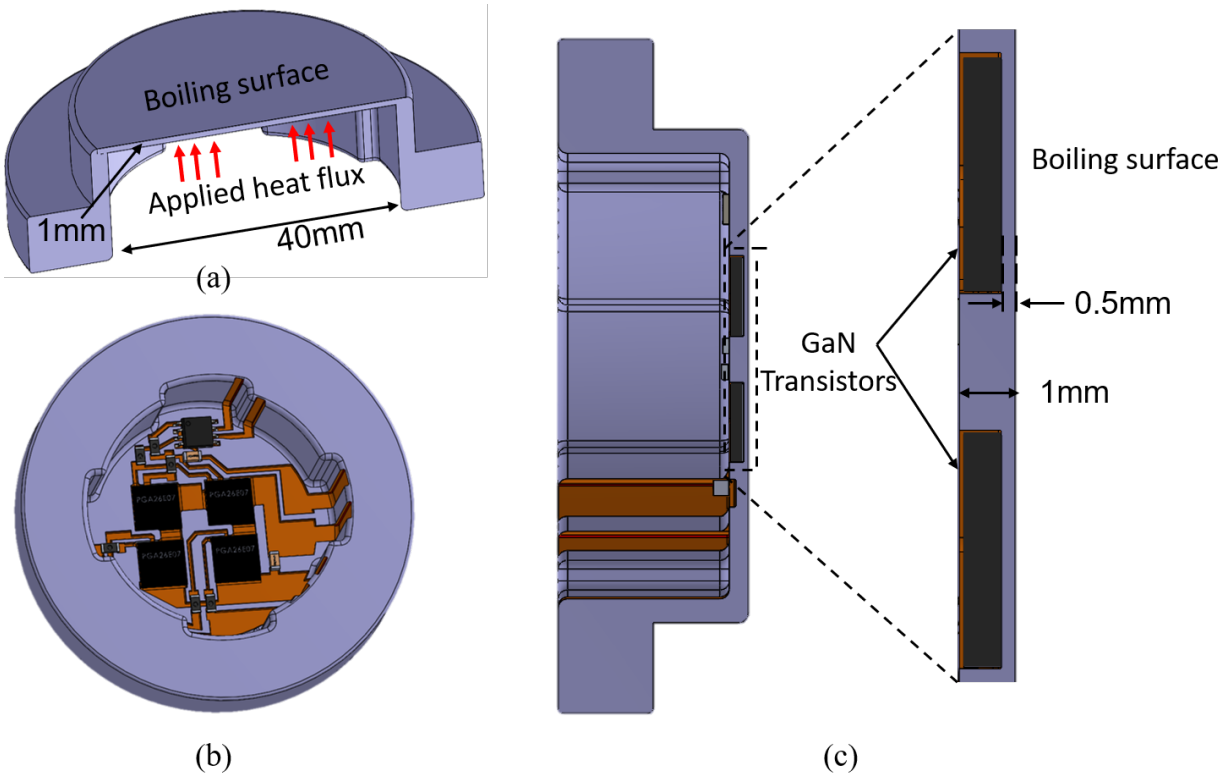

Figure 1: Design structure details of the 3D printed and copper metallized evaporator: (a) isometric section view, (b) bottom view, (c) cross section view.

Primary GaN-based circuit

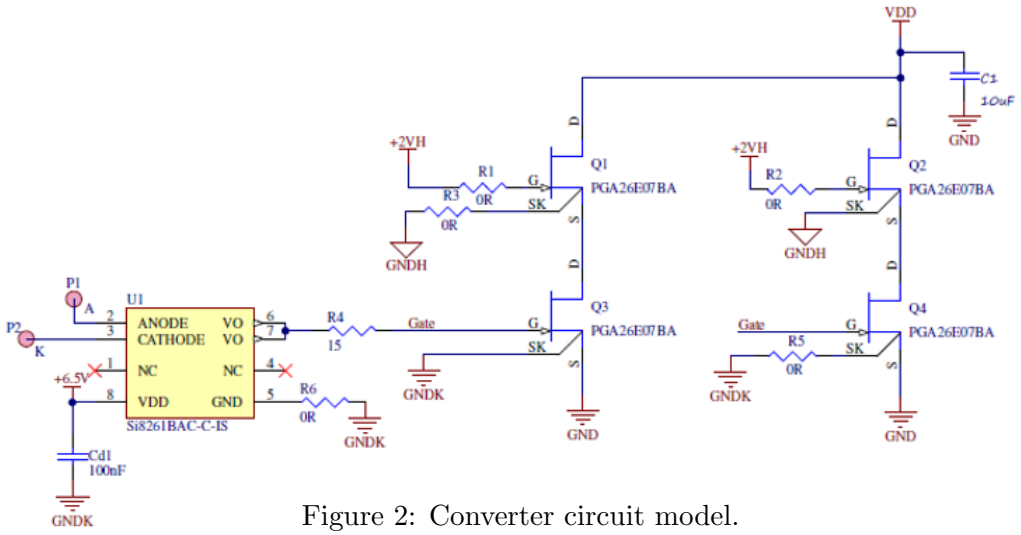

Figure 2: Converter circuit model.

The vehicle circuit is in fact made of dual legs (Fig. 2). The high-side GaN transistors are polarized as dissipating resistors. The gate resistors enable to slow the switching transient to accommodate the level of switching losses in addition to the steady-state losses due to the resistor-like transistors. This primary vehicle circuit is intended for the thermal analysis of the assembly and prior to any optimization of the floor-planning and geometrical circuit layout. The

quality of the switching of the transistors is not a primary concern as well as electro-magnetic interferences. The vehicle circuit is largely sufficient for providing losses with a heat flux up to 10 W/cm^2. The reason for using GaN transistors instead of discrete resistors is twofold: (i) it is necessary to take care of the transistor footprint to evaluate if the thermal assistance is preventing any hot spot and (ii) to verify the coherence of the fabrication of the converter. A hot spot would mean that the cooling effect is not homogeneous enough and that the thermal resistance between junction and ambient is not sufficiently lowered. The vehicle demonstrator is intended for experimental measurement of the effective heat transfer coefficient, h (W.m^{-2}.K^{-1}). This verification is required to prove the acceptability of the concept (significantly high coefficient value) and evaluate the power rating of the power core that can be thermally assisted using the proposed scheme and given a conservative energy efficiency attached to the electrical operation and a maximum temperature rise.

Fabrication of 3D-printed and metallized evaporator

The evaporator is 3D-printed with a Stereolithography (SLA) printer Form 2 from Formlabs (Fig. 3(a)). The high temperature resin FLHTAM01 from Formlabs is used for its thermal characteristics, i.e. it supports higher temperature compared to other available resins. After printing, the part is cleaned in isopropanol to remove resin residuals and then UV cured with thermal post-processing to enhance its mechanical strength. The polymer thermal diffusivity is measured with a flash method at $\alpha p = 1.7 \times 10^{-7}$ m^2/s. The surface roughness Sa is verified using an optical profilometer and is less than 2 μm.

The device is metallized by Electroless Deposition (ELD) of copper in a standard industrial process (method detailed in [16]). Briefly, this consists in immersing the evaporator in a palladium catalyst solution (Macuplex Activator-D34C, MacDermid), rinsing in water, and then plating in an electroless copper bath (Mid Copper 100XB, MacDermid) for about 2 hours. The process is quite long for safety reason with respect to the quality of copper. The process recipe may be optimized afterwards. As a result, the surface of the part where the palladium was deposited is metallized with copper (Fig. 3(b)) up to 7 μm in thickness as measured by X-ray fluorescence with a Bowman (Serial B-XRF). The electroless copper resistivity of the samples is measured with four-point-probe method and is equal to 2.2 $\mu\Omega$.cm, a value close to the resistivity of pure copper, which is 1.72 $\mu\Omega$.cm. Finally, the electronic components are soldered on the metallized part (Fig. 3(c)). For future application, copper thickening of the tracks by electrolytic Cu plating could be used to significantly increase the thickness and improve the electrical conductivity especially for high current ratings. The Cu thickness has not a significant impact on the thermal characteristics of the assembly so it is not further discussed here.

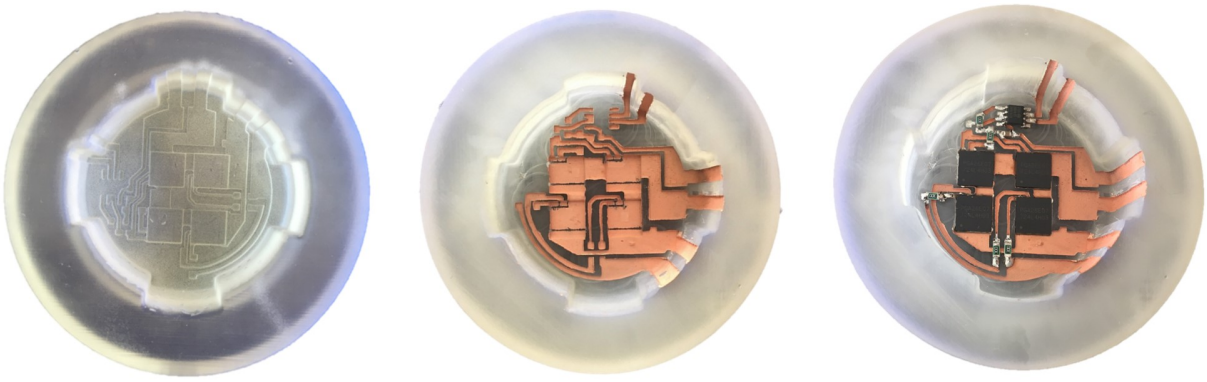

(a) (b) (c)

Figure 3: Images of the evaporator fabrication steps: (a) 3D printed evaporator, (b) Electroless copper plating of electronic circuit, (c) Soldering of the components.

Thermal characterization

An evaluation is conducted of the cooling performance of the evaporator in the case of heat dissipation using pool boiling of a fluid on its upper internal surface. To this end, as represented in Fig.4, the evaporator is tightly set into a sample holder, which is secured on a fixed mounting. A thermostatic transparent glass enclosure is then clamped at the base in order to seal the cavity. Several nitrile O-rings are used to ensure the airtightness of the assembly. One tiny K-Type thermocouple is attached to each of the dissipative electronic components to evaluate their local temperature with respect to residual possible hot spot location. In addition, two K-type thermocouples are placed directly within the enclosure to measure the fluid temperature. The first one, noted as T_1, is placed in the liquid phase while the second (T_v) is set in the vapor volume. Air is evacuated from the apparatus with the help of a vacuum pump to achieve a pressure lower than 500 Pa, and then partially filled with HFE7000 through the filling port represented in Fig. 4.

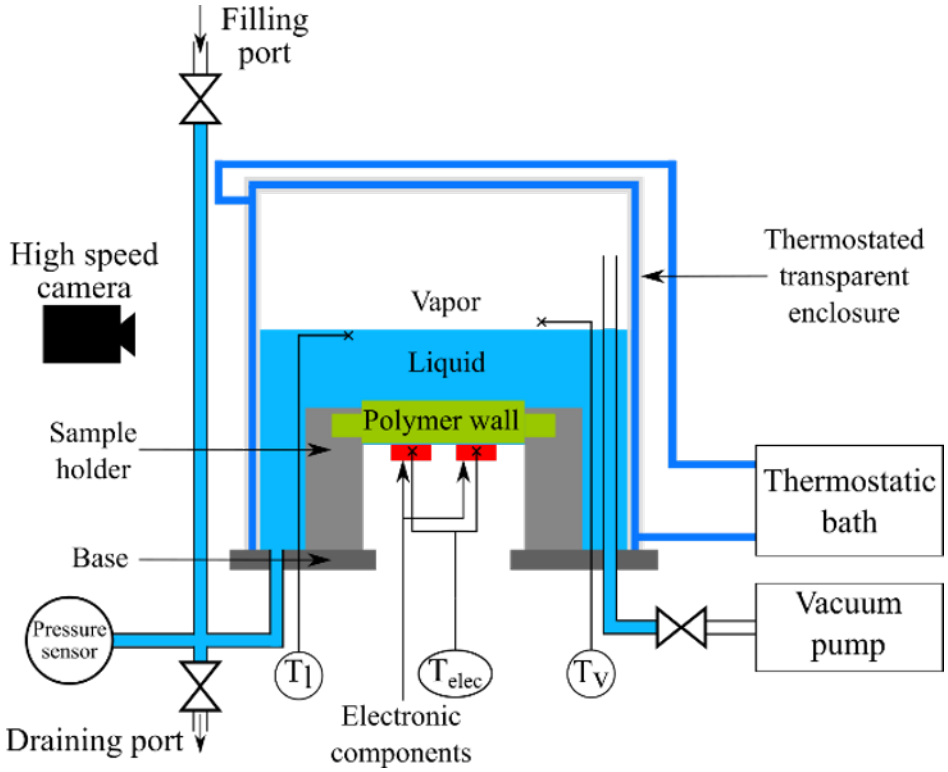

Figure 4: Schematic view of the experimental bench and associated sensors.

To evaluate the efficiency of two-phase cooling, the heat flux applied to the evaporator is sequentially increased until the electronic components reaches a maximum temperature of 130°C. The condition of maximum temperature, related to a local hot spot at the location of the GaN transistors, was reached before the critical heat flux (CHF) of boiling. At CHF, vapor generation is such that the liquid no longer wets the wall properly. The wall is then covered with a film of vapor and its temperature suddenly increases to stabilize itself at a very high value. CHF corresponds to the transition from the nucleate boiling regime to a film boiling regime, which is very stable. In the present experiments, the heat flux was sequentially decreased after reaching a peak value as explained before. At every step, the acquisition of data is started once a steady state is achieved. The apparent heat transfer coefficient, including the effect of heat conduction through the wall between the electronic component and the fluid, is then calculated as:

$$h_{app} = \frac{\phi_{elec}}{S \times \left(\bar{T}_{elec} - T_{sat}\right)} \tag{1}$$

where ϕ_{elec} is the total heat flux dissipated by the components, S is the total evaporator surface

area in contact with the dissipative components and $\bar{T}_{elec}$ is the mean value of the 4 components' temperature measurements. T_{sat} is deduced from the measured absolute pressure in the enclosure. This heat dissipation device as described above was designed for the cooling of GaN transistors, although it can be used for different types of electronic components.

In the following section, for measurement purposes and the sake of demonstration, the GaN transistors were replaced by low-profile, small footprint resistors. The variation of the apparent heat transfer coefficient with the effective heat flux density $\phi_{eff} = \phi_{elec}/S$ is represented in Fig. 5(a), on which the arrows indicate the increasing and decreasing heat flux cases. A slight hysteresis is observed, as the heat transfer coefficient is slightly higher when the heat flux is decreased from its maximum value. This small hysteresis can be correlated to the activation of the nucleation sites on the heated wall. Indeed, during the increasing heat flux phase, the phase change is not initiated at the lowest heat flux density values (up to $\phi_{eff} \approx 1.6$ W.cm^{-2}). Then, nucleate boiling is successively initiated on the surface corresponding to each of the dissipative elements. Boiling is fully developed above each component at a heat flux density of $\phi_{eff} \approx 3$ W.cm^{-2}. Indeed, as represented in Fig. 5(b), once the maximum heat flux density is achieved ($\phi_{eff} = 3.5$ W.cm^{-2}), the four areas facing the component are entirely covered by active nucleation sites.

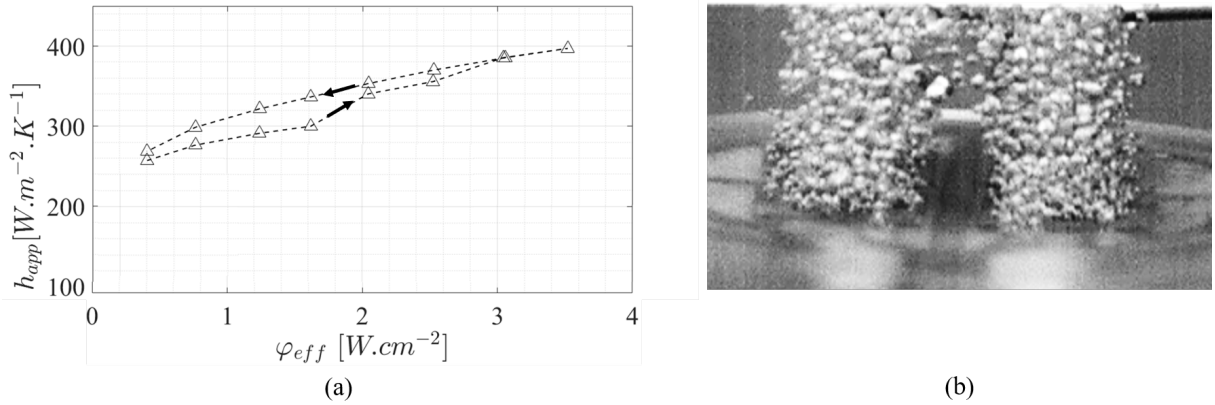

Figure 5: Thermal measurements: (a) Apparent heat transfer coefficient as a function of the effective heat flux density, (b) Nucleate boiling visualization on the polymer evaporator, $\phi_{eff} = 3.5$ W.cm^{-2}.

The evaporator was then tested with the GaN transistors circuit design, and its effectiveness was found to be the same. Although the temperatures could not be measured with accuracy, nucleate boiling was observed on the polymer evaporator indicating that the heat dissipation is effective.

It is noteworthy that the surface morphology has an important effect on the nucleate boiling performance. For example, increasing the roughness on the heat-dissipating surface, or creating geometric structures on it, can increase the number of active nucleation sites by trapping vapor nuclei and therefore improve the nucleate boiling performance [17]. Furthermore, the pinholes are regions where the thickness of the polymer wall is reduced and consequently, the wall temperature and the wall superheat are higher. Due to this higher superheat, the bubbles growth is further enhanced. To this end, a second 3D printed evaporator with pinholes was designed and fabricated (Fig. 6(a)). The pinholes with a radius of 500 μm, a depth of 300 μm and a 1000 μm pitch were placed on the boiling surface side, precisely at the location of the 4 components. The experimental results (Fig.6(b)) show that the apparent heat transfer coefficient increases under the effect of pinholes onto the boiling surface and that the maximum heat flux density is now 4.3 W.cm^{-2}.

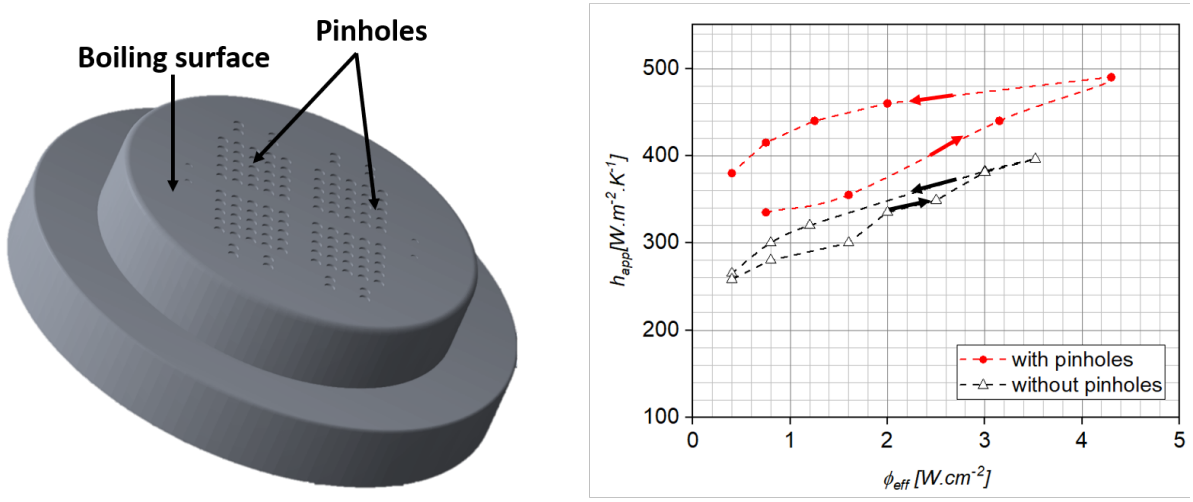

(a) (b)

Figure 6: 3D printed evaporator with pinholes on the boiling surface: (a) Boiling surface details, (b) Apparent heat transfer coefficient as a function of the effective heat flux density.

Future work

A second prototype with a classical power circuit has been fabricated using different options regarding the generation of nucleation sites and the selection of the polymer material for an enhanced thermal conductivity. Fig. 7(b) illustrates a prototype to be experimentally verified. The electrical circuit of this prototype is based on two independent inverter legs with independent gate drivers (Fig. 7(a)). This configuration enables to operate most DC/DC conversion topologies. GaN Systems (GS66508T) have been used in this prototype. The objective of the electro-thermal characterization is to evaluate the behavior of the system in a standard operating mode. The electrical behavior will make losses fluctuate among transistors and one interest is to evaluate thermal couplings. One other interest is to evaluate the behavior of the thermal part in the case of non-repetitive peak electrical operation to explore the design specifications of the evaporator with respect to the electrical specifications. The experimental validation of this second prototype is not available at the time of completing the edition of this paper.

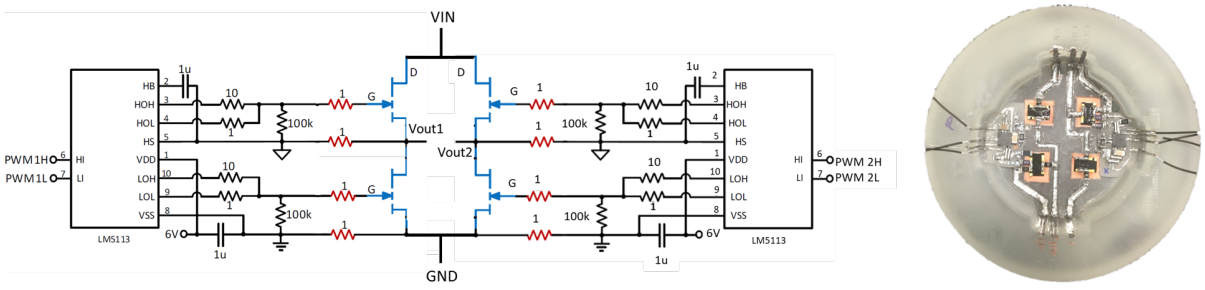

(a) (b)

Figure 7: Future prototype: (a) Electrical circuit based on two independent voltage legs with independent gate drivers, (b) one of the fabricated prototypes.

Conclusion

In this paper, a polymer-based heat-pipe evaporator for GaN transistors using AM and plastronics technology is fabricated and characterized. The use of polymer for heat pipes allows reducing the weight and cost of the assembly and improving their chemical compatibility with the cooling fluid. The copper circuit receiving the electronic components, is directly fabricated

on the polymer surface. The copper thickness and the electrical resistivity provide a sufficient conductivity for the circuit operation. However, the electrical conductivity could be improved using electrolytic Cu plating to adapt to high current rating. A specific test bench was developed to characterize the effective heat transfer between the polymer wall and the heat pipe working fluid. Based on the observations of the two-phase flow, a fully developed boiling regime can be achieved on this particular type of material. This allows to improve the overall thermal performance of the evaporator.

References

[1] D. Maier et al., "Testing the Temperature Limits of GaN-Based HEMT Devices," IEEE Trans. Device Mater. Reliab., vol. 10, no. 4, pp. 427–436, 2010.

[2] Y. Won, J. Cho, D. Agonafer, M. Asheghi, and K. E. Goodson, "Cooling limits for GaN HEMT technology," Tech. Dig. - IEEE Compd. Semicond. Integr. Circuit Symp. CSIC, no. February 2019, 2013, doi: 10.1109/CSICS.2013.6659222.

[3] Attaran, M.. "The rise of 3-D printing: The advantages of additive manufacturing over traditional manufacturing." Business Horizons 60 (2017): 677-688.

[4] Z. Yan, G. Liu, J. M. Khan, and A. A. Balandin, "Graphene quilts for thermal management of high-power GaN transistors," Nat. Commun., vol. 3, no. May, 2012, doi: 10.1038/ncomms1828.

[5] R. Kempers, J. Colenbrander, W. Tan, R. Chen, and A. J. Robinson, "Experimental characterization of a hybrid impinging microjet-microchannel heat sink fabricated using high-volume metal additive manufacturing," Int. J. Thermofluids, vol. 5–6, 2020, doi: 10.1016/j.ijft.2020.100029.

[6] M. T. Ababneh, C. Tarau, and W. G. Anderson, "0DQDJHPHQW," 2019 18th IEEE Intersoc. Conf. Therm. Thermomechanical Phenom. Electron. Syst., pp. 656–665, 2019.

[7] S. Ozguc, S. Pai, L. Pan, G. Patrick, and J. Weibel, "Experimental Demonstration of an Additively Manufactured Vapor Chamber Heat Spreader," 18th IEEE ITHERM Conf., vol. 2, 2019.

[8] Z. Hu, D. Wang, J. Xu, and L. Zhang, "Development of a loop heat pipe with the 3D printed stainless steel wick in the application of thermal management," Int. J. Heat Mass Transf., vol. 161, p. 120258, 2020, doi: 10.1016/j.ijheatmasstransfer.2020.120258.

[9] M. Chinthavali, Z. J. Wang, S. Campbell, T. Wu, and B. Ozpineci, "50-kW 1kV DC bus air-cooled inverter with 1.7 kV SiC MOSFETs and 3D-printed novel power module packaging structure for grid applications," Conf. Proc. - IEEE Appl. Power Electron. Conf. Expo. - APEC, vol. 2018-March, pp. 133–140, 2018, doi: 10.1109/APEC.2018.8340999.

[10] A. Michalak et al., "A Thermal Management Design Methodology for Advanced Power Electronics Utilizing Genetic Optimization and Additive Manufacturing Techniques," Intersoc. Conf. Therm. Thermomechanical Phenom. Electron. Syst. ITHERM, vol. 2020-July, pp. 547–557, 2020, doi: 10.1109/ITherm45881.2020.9190444.

[11] T. W. Wei et al., "Demonstration of Package Level 3D-printed Direct Jet Impingement Cooling applied to High power, Large Die Applications," Proc. - Electron. Components Technol. Conf., vol. 2020-June, pp. 1422–1429, 2020, doi: 10.1109/ECTC32862.2020.00225.

[12] B. Kwon, T. Foulkes, T. Yang, N. Miljkovic, and W. P. King, "Air Jet Impingement Cooling of Electronic Devices Using Additively Manufactured Nozzles," IEEE Trans. Components, Packag. Manuf. Technol., vol. 10, no. 2, pp. 220–229, 2020, doi: 10.1109/TCPMT.2019.2936852.

[13] M. Smith et al., "Maximizing the performance of a 3D printed heat sink by accounting for anisotropic thermal conductivity during filament deposition," Intersoc. Conf. Therm. Thermomechanical Phenom. Electron. Syst. ITHERM, vol. 2019-May, pp. 626–632, 2019, doi: 10.1109/ITHERM.2019.8757285.

[14] Y. Xu and C. Deng, "An investigation on 3D printing technology for power electronic converters," 2017 IEEE 8th Int. Symp. Power Electron. Distrib. Gener. Syst. PEDG 2017, 2017, doi: 10.1109/PEDG.2017.7972486.

[15] F. Jorg, "Three-Dimensional Molded Interconnect Devices (3D-MID)," Three-Dimensional Molded Interconnect Devices (3D-MID), pp. I–XII, 2014, doi: 10.3139/9781569905524.fm.

[16] T. Gerges, V. Semet, P. Lombard, S. Gaillard, M. Cabrera, and S. A. Lambert, "3D Plastronics for Smartly Integrated Magnetic Resonance Imaging Coils," Front. Phys., vol. 8, no. July, pp. 1–13, 2020, doi: 10.3389/fphy.2020.00240.

[17] J. Kim, S. Jun, R. Laksnarain, and S. M. You, "Effect of surface roughness on pool boiling heat transfer at a heated surface having moderate wettability," Int. J. Heat Mass Transf., vol. 101, pp. 992–1002, 2016, doi: 10.1016/j.ijheatmasstransfer.2016.05.067.